

# Influence of momentum-dependent interactions on balance energy and mass dependence<sup>\*</sup>

A.D. Sood and R.K. Puri<sup>a</sup>

Physics Department, Panjab University, Chandigarh -160 014, India

Received: 20 July 2006 / Revised: 4 October 2006 /

Published online: 22 December 2006 – © Società Italiana di Fisica / Springer-Verlag 2006

Communicated by Th. Walcher

**Abstract.** We aim to understand the role of momentum-dependent interactions in transverse flow as well as in its disappearance. For the present study, central collisions involving masses between 24 and 394 are considered. We find that the momentum-dependent interactions have different impact in lighter colliding nuclei compared to heavier colliding nuclei. In lighter nuclei, the contribution of the mean field towards flow is smaller compared to heavier nuclei where binary nucleon-nucleon collisions dominate the scene. The inclusion of momentum-dependent interactions also explains the energy of the vanishing flow in the  $^{12}\text{C} + ^{12}\text{C}$  reaction which otherwise was not possible with the static hard equation of state. An excellent agreement of our theoretical attempt is found for balance energy with experimental data throughout the periodic table.

**PACS.** 25.70.Pq Multifragment emission and correlations – 25.70.-z Low and intermediate energy heavy-ion reactions

## 1 Introduction

One of the major goals of heavy-ion collisions at intermediate energies is to study the properties of hot and dense nuclear matter formed during a collision. The nuclear-matter equation of state (EOS) has attracted a lot of attention over the past two decades because of its wider usefulness in several branches of physics [1]. Apart from the equation of state, its momentum dependence has also been of great concern because of its larger influence on the dynamics and observables of heavy-ion collisions. The initial attempts with momentum-dependent interactions (MDI) showed drastic effects on the collective flow as well as on the particle production [2,3]. The pion yields were found to be suppressed by as much as 30% in the presence of momentum-dependent interactions [2]. Interestingly, momentum-dependent interactions also suppressed the nucleon-nucleon collisions by the same amount. This happened because of the fact that the inclusion of momentum-dependent interactions accelerate the nucleons in the transverse direction during the initial phase of the reaction. This leads the matter to a lower density resulting in fewer nucleon-nucleon collisions. Similarly, if one goes from the soft to the hard equation of state, the pion yield was reported to be reduced by  $\approx 10\%$ . Interestingly, a soft equation of state with momentum-dependent

interactions (SMD) yields the same transverse momentum as a static hard equation of state [2,3]. In some studies [4, 5], the SMD equation of state was reported to explain the data better than the hard equation of state.

Khoa *et al.* [6] also showed that the inclusion of momentum-dependent interactions leads to a reduced nuclear density and temperature whereas transverse momentum observes a reverse trend. From the above discussions, it is clear that the momentum dependence of the nuclear mean field plays a major role in determining the nuclear dynamics and is an important feature for the fundamental understanding of the nuclear-matter properties over a wide range of densities and temperatures.

Various theoretical attempts were made within the framework of either the Boltzmann-Uehling-Uhlenbeck (BUU) model [3–5,7–14] or the quantum molecular dynamics (QMD) model [2,6,15–17]. One has also tried to understand the influence of momentum-dependent interactions on the flow as well as on its disappearance using a variety of nucleon-nucleon cross-sections along with different static equations of state. These observables were thought to shed light on the nature of the equation of state as well as on the strength of the nucleon-nucleon cross-section. However, if one looks carefully in the literature, one finds that one has often taken one or two reactions and tried to conclude about the above-cited problems. The need of the hour is to look beyond one or two reactions. We shall here concentrate on the role of

<sup>\*</sup> Part of a PhD Thesis by A.D. Sood

<sup>a</sup> e-mail: rkpuri@pu.ac.in

momentum-dependent interactions in collective transverse flow as well as in its disappearance in heavy-ion collisions throughout the periodic table. Moreover, the conclusions of several authors are also contradictory to each other sometimes. For example, the flow values using the SMD equation of state are higher compared to those using the hard equation of state for  $^{93}\text{Nb} + ^{93}\text{Nb}$  and  $^{40}\text{Ca} + ^{40}\text{Ca}$  reactions at 400 MeV/nucleon [5,6]. However, a reverse observation was reported for  $^{197}\text{Au} + ^{197}\text{Au}$  reactions at 400 and 800 MeV/nucleon [18]. Interestingly, some studies showed the same flow values for the SMD and hard equations of state [2–4,6]. On the contrary, refs. [9,10] showed the insensitive nature of flow towards the equation of state irrespective of the momentum-dependent interactions.

Further, some studies [6] demonstrated that the soft equation of state gives a larger flow compared to the hard equation of state whereas others [6,7,18] claimed (for  $^{197}\text{Au} + ^{197}\text{Au}$  reactions at 200–800 MeV/nucleon,  $^{93}\text{Nb} + ^{93}\text{Nb}$  at 400 MeV/nucleon, and  $^{139}\text{La} + ^{139}\text{La}$  at 800 MeV/nucleon, respectively) just the reverse. Reference [5] demonstrated a better agreement with the data using SMD for the Ar + Pb reaction, whereas ref. [18] concluded just the opposite for the  $^{197}\text{Au} + ^{197}\text{Au}$  reaction.

Apart from the collective flow, the balance energy ( $E_{bal}$ ) (the incident energy at which the transverse flow disappears) also faces similar contradictions for different equations of state [19–21]. All the above-mentioned examples indicate the need for a systematic study of the influence of momentum-dependent interactions on the flow as well as on its disappearance throughout the periodic table. This may also pin down the above-mentioned questions and one may also get a universal behavior of the momentum-dependent interactions in the disappearance of flow.

It is worth mentioning that the mass dependence studies have always been performed in different problems of heavy-ion physics. For example, the mass dependence in the evolution of density and temperature reveals that the maximum density scales with the size of the system [6,7,22] whereas the maximum temperature is insensitive towards the mass of the system. Similarly, multifragmentation, particle production, as well as collective flow (the most sensitive observable) also depend strongly on the mass of the system. Therefore, any agreement/disagreement with experimental observations depends upon the size of the reacting partner. In our previous work [23], we presented a complete theoretical analysis of the balance energy using the QMD model, where the model was confronted with the balance energy observed in the following reactions:  $^{20}\text{Ne} + ^{27}\text{Al}$  [24],  $^{36}\text{Ar} + ^{27}\text{Al}$  [25,26],  $^{40}\text{Ar} + ^{27}\text{Al}$  [19],  $^{40}\text{Ar} + ^{45}\text{Sc}$  [16,24,27],  $^{40}\text{Ar} + ^{51}\text{V}$  [20,28],  $^{64}\text{Zn} + ^{27}\text{Al}$  [21],  $^{40}\text{Ar} + ^{58}\text{Ni}$  [29],  $^{64}\text{Zn} + ^{48}\text{Ti}$  [26],  $^{58}\text{Ni} + ^{58}\text{Ni}$  [13,27,29,30],  $^{58}\text{Fe} + ^{58}\text{Fe}$  [13,30],  $^{64}\text{Zn} + ^{58}\text{Ni}$  [26],  $^{86}\text{Kr} + ^{93}\text{Nb}$  [24,27],  $^{93}\text{Nb} + ^{93}\text{Nb}$ [31],  $^{129}\text{Xe} + ^{118}\text{Sn}$  [29],  $^{139}\text{La} + ^{139}\text{La}$  [31], and  $^{197}\text{Au} + ^{197}\text{Au}$  [27,32,33]. Apart from the above-mentioned and extensively analyzed reactions, the discussion about the  $^{12}\text{C} + ^{12}\text{C}$  reaction is

often omitted [24]. Therefore, one also needs to understand the dynamics involved in the balance energy of the  $^{12}\text{C} + ^{12}\text{C}$  system. As mentioned above, some attempts are made in the literature to study the balance energy with momentum-dependent interactions [14,17]. However, barring ref. [14], no attempt exists in the literature where mass dependence of the balance energy is studied using momentum-dependent interactions. The mass dependence of the balance energy and other variables using momentum-dependent interactions may have an interesting physics since the surface contribution in the lighter nuclei is much larger compared to the heavier ones. For example, the ratio of the surface to the radius is 0.12 in the  $^{12}\text{C} + ^{12}\text{C}$  system whereas it is 0.022 in the  $^{197}\text{Au} + ^{197}\text{Au}$  system (the surface is defined as the radial distance marked with density between 90% and 10% of its central value, whereas the radius is the distance where the density falls to 50% of the central density). In other words, the surface effects and surface to volume ratio will be much stronger in the light nuclei compared to the heavy ones, giving us a possibility to examine the role of momentum-dependent interactions at wider scale.

Our present aim, therefore, is at least twofolds.

1) To study the collective transverse flow and its disappearance in the collision of  $^{12}\text{C} + ^{12}\text{C}$ .

2) To understand the role of momentum-dependent interactions in the collective transverse flow as well as in its disappearance throughout the periodic table in central collisions. Further, to analyze whether the mass dependence of the balance energy using momentum-dependent interactions can be parameterized in terms of some scaling relations or not.

The present study is made within the framework of the QMD model, which is discussed briefly in sect. 2. The details of the model can be found in several previous studies [2,15,17,23,34–36]. Section 3 spells our results and sect. 4 summarizes the outcome.

## 2 The model

In the QMD model, each nucleon propagates under the influence of mutual two- and three-body interactions. The propagation is governed by the classical equations of motion:

$$\dot{\mathbf{r}}_i = \frac{\partial H}{\partial \mathbf{p}_i}; \quad \dot{\mathbf{p}}_i = -\frac{\partial H}{\partial \mathbf{r}_i}, \quad (1)$$

where  $H$  stands for the Hamiltonian which is given by

$$H = \sum_i^A \frac{\mathbf{p}_i^2}{2m_i} + \sum_i^A (V_i^{\text{Skyrme}} + V_i^{\text{Yuk}} + V_i^{\text{Coul}} + V_i^{\text{mdi}}). \quad (2)$$

Here  $V_i^{\text{Skyrme}}$ ,  $V_i^{\text{Yuk}}$ ,  $V_i^{\text{Coul}}$  and  $V_i^{\text{mdi}}$  are, respectively, the Skyrme, Yukawa, Coulomb and momentum-dependent potentials. The momentum-dependent interactions are obtained by parameterizing the momentum dependence of the real part of the optical potential. The final form of the potential reads as [2,34]

$$U^{\text{mdi}} \approx t_4 \ln^2[t_5(\mathbf{p}_1 - \mathbf{p}_2)^2 + 1]\delta(\mathbf{r}_1 - \mathbf{r}_2). \quad (3)$$

Here  $t_4 = 1.57 \text{ MeV}$  and  $t_5 = 5 \times 10^{-4} \text{ MeV}^{-2}$ . A parameterized form of the local plus mdi potential is given by

$$U = \alpha \left( \frac{\rho}{\rho_0} \right) + \beta \left( \frac{\rho}{\rho_0} \right) + \delta \ln^2 [\epsilon (\rho/\rho_0)^{2/3} + 1] \rho / \rho_0. \quad (4)$$

The parameters  $\alpha, \beta, \gamma, \delta$  and  $\epsilon$  are, respectively,  $-124, 70.5, 2, 0, 0$  for the hard EOS and  $-130, 59, 2.09, 1.57, 21.54$  for HMD. Following refs. [9, 10, 14–17, 19, 21, 23, 35, 37, 38], we here use a hard equation of state throughout. It should, however, be noted that the success rate is nearly the same for both soft and hard equations of state. As explained in ref. [23] and others [10, 19, 35, 38, 39], an isotropic and constant nucleon-nucleon cross-section between 40 and 55 mb is employed in the present study. In the light of ref. [40], the isospin dependence of the cross-section is neglected.

### 3 Results and discussion

We simulated 1000–3000 events for each  $^{12}\text{C} + ^{12}\text{C}$  ( $b/b_{max} = 0.4$ ),  $^{20}\text{Ne} + ^{27}\text{Al}$  ( $b/b_{max} = 0.4$ ),  $^{36}\text{Ar} + ^{27}\text{Al}$  ( $b = 2 \text{ fm}$ ),  $^{40}\text{Ar} + ^{27}\text{Al}$  ( $b = 1.6 \text{ fm}$ ),  $^{40}\text{Ar} + ^{45}\text{Sc}$  ( $b/b_{max} = 0.4$ ),  $^{40}\text{Ar} + ^{51}\text{V}$  ( $b/b_{max} = 0.3$ ),  $^{40}\text{Ar} + ^{58}\text{Ni}$  ( $b = 0\text{--}3 \text{ fm}$ ),  $^{64}\text{Zn} + ^{48}\text{Ti}$  ( $b = 2 \text{ fm}$ ),  $^{58}\text{Ni} + ^{58}\text{Ni}$  ( $b/b_{max} = 0.28$ ),  $^{64}\text{Zn} + ^{58}\text{Ni}$  ( $b = 2 \text{ fm}$ ),  $^{86}\text{Kr} + ^{93}\text{Nb}$  ( $b/b_{max} = 0.4$ ),  $^{93}\text{Nb} + ^{93}\text{Nb}$  ( $b/b_{max} = 0.3$ ),  $^{129}\text{Xe} + ^{Nat}\text{Sn}$  ( $b = 0\text{--}3 \text{ fm}$ ),  $^{139}\text{La} + ^{139}\text{La}$  ( $b/b_{max} = 0.3$ ), and  $^{197}\text{Au} + ^{197}\text{Au}$  ( $b = 2.5 \text{ fm}$ ) reactions using HMD and hard equations of state at various incident energies between 30 MeV/nucleon and 800 MeV/nucleon in small steps. Constant cross-sections between 40 and 55 mb strength are also used. The impact parameters are taken from the experimental extractions [13, 16, 19–21, 24–33]. The directed transverse momentum is calculated using  $\langle p_x^{dir} \rangle$  [17, 23, 34–36]:

$$\langle p_x^{dir} \rangle = \frac{1}{A} \sum_i \text{sgn}\{Y(i)\} p_x(i), \quad (5)$$

where  $Y(i)$  and  $p_x(i)$  are, respectively, the rapidity distribution and transverse momentum of the  $i$ -th particle.

In fig. 1, we display  $\langle p_x^{dir} \rangle$  as a function of the incident energy ranging between 30 MeV/nucleon and 800 MeV/nucleon. Here, the displayed reactions are  $^{12}\text{C} + ^{12}\text{C}$ ,  $^{40}\text{Ar} + ^{45}\text{Sc}$ ,  $^{93}\text{Nb} + ^{93}\text{Nb}$ , and  $^{197}\text{Au} + ^{197}\text{Au}$ . The open (solid) diamonds denote the  $\langle p_x^{dir} \rangle$  values for HMD (Hard) equation of state. A constant cross-section of 55 mb has been used in this figure. In all the cases, the transverse momentum is negative at smaller incident energies which turns positive at relatively higher incident energies. The value of the abscissa at zero value of  $\langle p_x^{dir} \rangle$  corresponds to the energy of vanishing flow (EVF) or, alternatively, the balance energy ( $E_{bal}$ ). The following important results emerge from the graph.

1) The transverse momentum increases monotonically with the increase in the incident energy. The increase in the transverse flow  $\langle p_x^{dir} \rangle$  is sharp at smaller incident energies (up to 200 MeV/nucleon) compared to higher incident

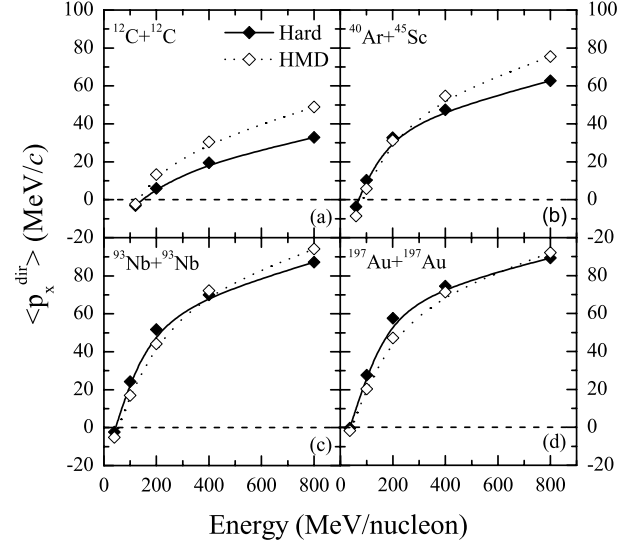


**Fig. 1.**  $\langle p_x^{dir} \rangle$  as a function of the incident energy for four different reactions: (a)  $^{12}\text{C} + ^{12}\text{C}$ , (b)  $^{40}\text{Ar} + ^{45}\text{Sc}$ , (c)  $^{93}\text{Nb} + ^{93}\text{Nb}$ , and (d)  $^{197}\text{Au} + ^{197}\text{Au}$ . Solid (open) diamonds represent the hard (HMD) equation of state. The lines are only to guide the eye. A constant nucleon-nucleon cross-section of 55 mb strength is used.

energies where it starts saturating. Its slope decreases at higher incident energies that finally saturates depending upon the mass of the colliding nuclei.

2) At higher energies (*e.g.*, above 400 MeV/nucleon) the repulsion due to momentum-dependent interactions is stronger during the early phase of the reaction and transverse momentum increases sharply. However, the overall effect depends on the mass of the colliding nuclei. The difference of  $\langle p_x^{dir} \rangle$  between HMD and hard equations of state decreases as one goes from the lighter to the heavier systems. For example, the difference ( $\langle p_x^{dir} \rangle_{HMD} - \langle p_x^{dir} \rangle_{Hard}$ ) at 400 MeV/nucleon is approximately, 11, 7.3, 2, and  $-3.2 \text{ MeV/c}$ , respectively, for the reactions  $^{12}\text{C} + ^{12}\text{C}$ ,  $^{40}\text{Ar} + ^{45}\text{Sc}$ ,  $^{93}\text{Nb} + ^{93}\text{Nb}$ , and  $^{197}\text{Au} + ^{197}\text{Au}$ . If one calculates the normalized percentage (*i.e.*,  $\{(\langle p_x^{dir} \rangle_{HMD} - \langle p_x^{dir} \rangle_{Hard}) / \langle p_x^{dir} \rangle_{Hard}\} \times 100$ ), these numbers are modified to 56.35, 15.44, 3.04, and  $-4.31\%$ , respectively, for the reactions  $^{12}\text{C} + ^{12}\text{C}$ ,  $^{40}\text{Ar} + ^{45}\text{Sc}$ ,  $^{93}\text{Nb} + ^{93}\text{Nb}$ , and  $^{197}\text{Au} + ^{197}\text{Au}$ . Note that the lighter colliding nuclei now show a huge variation compared to the heavy ones where effects are insignificant.

3) If one looks at the results in the vicinity of the balance energy, one sees that the momentum-dependent interactions suppress the transverse momentum and hence enhance the balance energy in agreement with refs. [15, 17]. The enhancement in the balance energy due to momentum-dependent interactions is, respectively, 13.29, 10.11, and 2.6 MeV/nucleon for the reactions of  $^{40}\text{Ar} + ^{45}\text{Sc}$ ,  $^{93}\text{Nb} + ^{93}\text{Nb}$ , and  $^{197}\text{Au} + ^{197}\text{Au}$ . On the contrary, momentum-dependent interactions reduce the energy of the vanishing flow in the  $^{12}\text{C} + ^{12}\text{C}$  reaction by 9.9 MeV/nucleon.

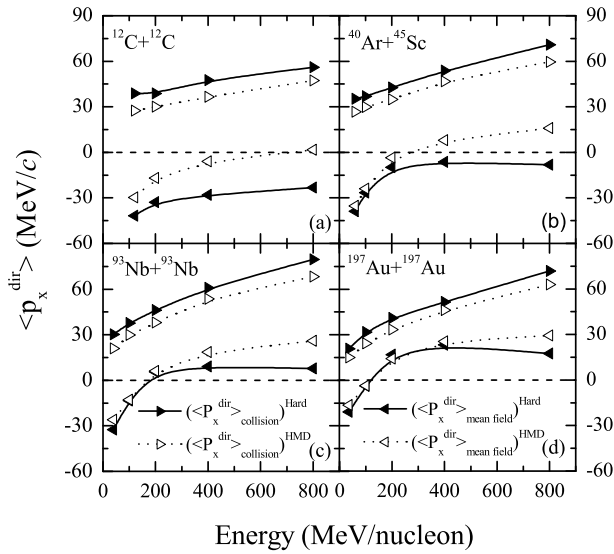


**Fig. 2.** The decomposition of  $\langle p_x^{dir} \rangle$  into mean field (left triangles) and collision part (right triangles) as a function of the incident energy. Again, solid (open) triangles represent the hard (HMD) equation of state.

All the above-mentioned findings can be understood by decomposing the total transverse momentum into the contributions due to mean-field and two-body nucleon-nucleon collisions (as shown in fig. 2). This decomposition has been explained in details in ref. [23]. The left triangles represent the mean-field contribution whereas the collision contribution is displayed by the right triangles. The open (solid) triangles represent the HMD (Hard) equation of state. One notices that the flow due to binary nucleon-nucleon collisions increases almost linearly with the increase in the incident energy in all the above-listed reactions. The mean-field flow, however, increases sharply up to a couple of hundred MeV/nucleon, then it saturates. This trend is slower in the lighter colliding nuclei compared to the heavy ones. In other words, the continuous increase in the total transverse momentum in high-energy tail results due to the frequent nucleon-nucleon binary collisions alone. Under this saturation, the overall trend of the role of momentum-dependent interactions in transverse flow is decided by the impact of the mean field. The striking result is for the case of the  $^{12}\text{C} + ^{12}\text{C}$  reaction, where the contribution of the mean field towards collective transverse flow using momentum-dependent interactions dominates the decrease in the collective flow due to nucleon-nucleon collisions using momentum-dependent interactions resulting in the net increased transverse flow due to HMD compared to the static equation of state. Whereas, for medium-mass nuclei (*e.g.*,  $^{93}\text{Nb} + ^{93}\text{Nb}$ ), the increase in flow due to mean field is almost balanced by the decrease in flow due to nucleon-nucleon binary collisions, therefore neutralizing the net effect. For the heavier systems, a very little swing can be noticed. In other words, the role of momentum-dependent interactions in the mean-field contribution depends on the mass of the system. In lighter systems, the role of momentum-dependent interactions is larger but decreases for the heavier colliding nuclei.

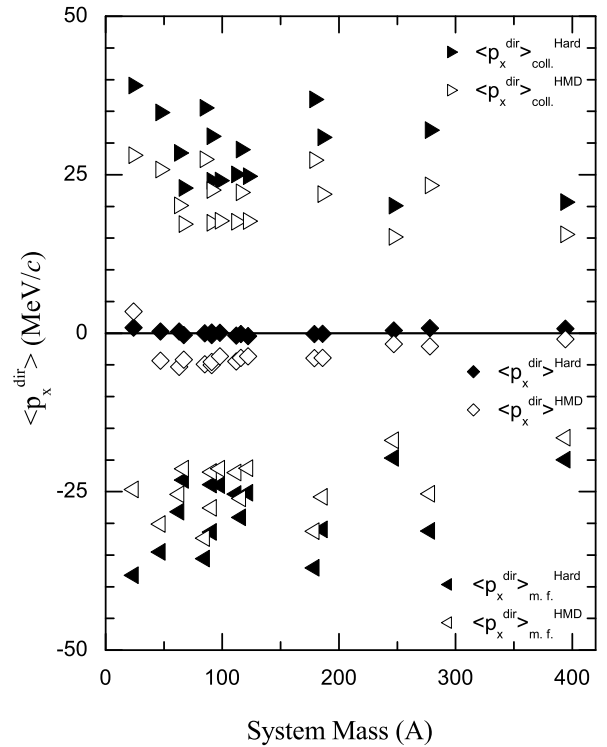


**Fig. 3.** Total  $\langle p_x^{dir} \rangle$  (diamonds) and its decomposition into mean field (left triangles) and collision part (right triangles) as a function of the mass of the system at the balance energy of the hard equation of state. Solid (open) symbols represent the hard (HMD) equation of state.

Let us now examine the mass dependence of the momentum-dependent interactions in the balance energy  $\rightarrow A$  point in the energy scale corresponding to the vanishing flow. A careful look at fig. 2 shows that the balance energy is, respectively, 142.88 (133), 70.11 (83.4), 47.18 (57.29), and 37.44 (40.1) MeV/nucleon for the reactions  $^{12}\text{C} + ^{12}\text{C}$ ,  $^{40}\text{Ar} + ^{45}\text{Sc}$ ,  $^{93}\text{Nb} + ^{93}\text{Nb}$ , and  $^{197}\text{Au} + ^{197}\text{Au}$  using Hard (HMD). All the reactions, except  $^{12}\text{C} + ^{12}\text{C}$ , show a uniform trend, *i.e.*, the inclusion of momentum-dependent interactions reduces the transverse flow at low incident energies, therefore pushing the balance energy towards higher end. However, the  $^{12}\text{C} + ^{12}\text{C}$  reaction shows just the opposite. To understand this, let us divide the total transverse momentum at the energy of vanishing flow into contributions resulting from the mean field as well as collision parts. In fig. 3, we plot the decomposition for all the reactions reported in the introduction where the balance energy has been measured and reported experimentally. As discussed above, the difference between the transverse-flow contributions due to mean field of HMD and hard equations of state is maximal for lighter colliding nuclei but gets suppressed for the heavier colliding nuclei.

It was argued by Zhou *et al.* [14] that for the lighter systems like  $^{12}\text{C} + ^{12}\text{C}$ , a larger value of the balance energy results in a stronger momentum-dependent repulsion that enhances the transverse momentum and hence suppresses the balance energy. Our findings are also pointing

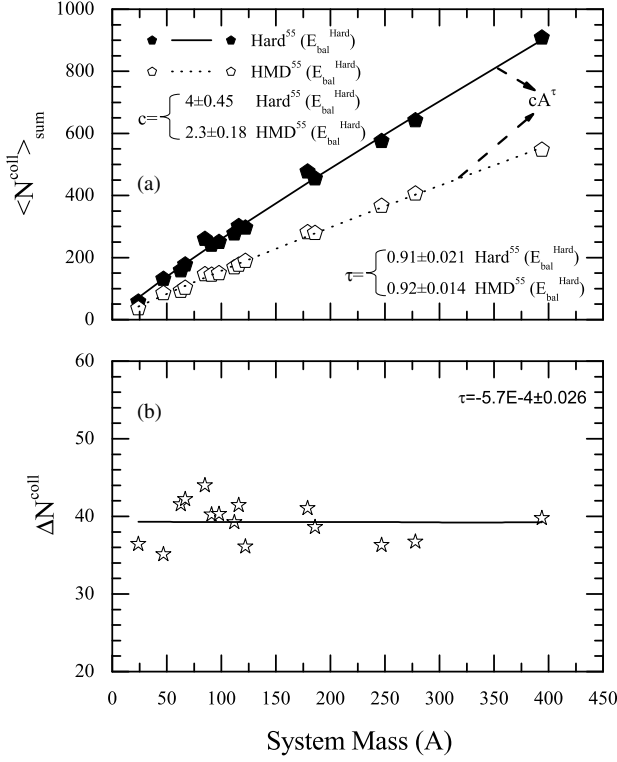


**Fig. 4.** (a) The total number of allowed nucleon-nucleon collisions as a function of the total mass of the system at the balance energy of the hard equation of state. Solid (open) pentagons represent the hard (HMD) equation of state. The lines are a power law fit of the form  $cA^\tau$ . The solid (dotted) line represents the power law fit for the hard (HMD) equation of state. (b) The percentage difference  $\Delta N^{coll}$  as a function of the mass of the system.

towards the same effects. However, one should also keep in the mind that this trend is not universal in the mass range. Looking at fig. 1, one notices that the collisions of heavier colliding nuclei at the balance energy of the  $^{12}\text{C} + ^{12}\text{C}$  reaction do not yield any significant difference or trend shown by the  $^{12}\text{C} + ^{12}\text{C}$  reaction.

Let us check whether the inclusion of momentum-dependent interactions reduces the frequency of nucleon-nucleon binary collisions or not. We display in fig. 4a, the total number of nucleon-nucleon collisions observed in the simulations using HMD and hard equations of state as a function of the mass of the system at the balance energy of the hard equation of state. The aim to simulate the reaction of HMD also at the balance energy of the static hard equation of state is to eliminate any variation that might result due to a different balance energy in HMD compared to that in the hard equation of state. The solid line corresponds to the hard equation of state, whereas the dotted line shows the outcome for the HMD equation of state. As is evident, the inclusion of momentum-dependent interactions suppresses the binary collisions by as much as 35–45% throughout the mass range which is in close agreement with ref. [2]. Further, these can be parameterized by a power law of the form  $cA^\tau$  with  $\tau = 0.92 \pm 0.014$

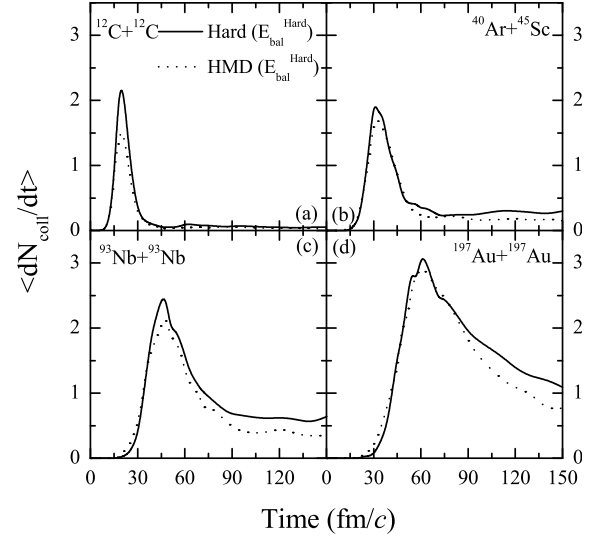


**Fig. 5.** The rate of allowed nucleon-nucleon collisions  $dN_{coll}/dt$  versus reaction time for the reactions (a)  $^{12}\text{C} + ^{12}\text{C}$ , (b)  $^{40}\text{Ar} + ^{45}\text{Sc}$ , (c)  $^{93}\text{Nb} + ^{93}\text{Nb}$  and (d)  $^{197}\text{Au} + ^{197}\text{Au}$ . Solid (dotted) lines represent the hard (HMD) equation of state.

and  $\tau = 0.91 \pm 0.021$ , respectively, for the HMD and the hard equation of state. The similar value of the power law parameter  $\tau$  points towards the universal suppression of binary collisions due to the inclusion of momentum-dependent interactions. To look more carefully, we plot in fig. 4b the percentage difference of binary nucleon-nucleon collisions defined as

$$\Delta N^{coll} = \left| \frac{\langle N^{coll} \rangle_{HMD} - \langle N^{coll} \rangle_{Hard}}{\langle N^{coll} \rangle_{Hard}} \right| \times 100. \quad (6)$$

As stated above, we see that the average suppression is of the order of 40% throughout the periodic-table masses.

Since the above discussion was for the final-stage collisions, it will be of further interest to see how collisions are affected during the course of the reaction. To see how momentum-dependent interactions can affect the frequency of the binary collisions, we show in fig. 5 the rate of change of allowed collisions,  $dN/dt$ , as a function of time for  $^{12}\text{C} + ^{12}\text{C}$ ,  $^{40}\text{Ar} + ^{45}\text{Sc}$ ,  $^{93}\text{Nb} + ^{93}\text{Nb}$ , and  $^{197}\text{Au} + ^{197}\text{Au}$ . This rate is after eliminating the Pauli-blocked collisions. Interestingly, during the early phase of the reaction, the inclusion of momentum-dependent interactions has a drastic effect on the collision rate compared to the hard equation of state in lighter colliding nuclei. This trend is reversed in the case of heavier nuclei where very little effect can be seen. This also points towards the stronger effect of momentum-dependent interactions in lighter nuclei compared to heavy colliding nuclei. This is perhaps due to Pauli blocking of final-stage collisions.

To understand the suppression of the flow using momentum-dependent interactions, we display in fig. 6 the time evolution of the rescaled density, for the reactions  $^{12}\text{C} + ^{12}\text{C}$ ,  $^{40}\text{Ar} + ^{45}\text{Sc}$ ,  $^{93}\text{Nb} + ^{93}\text{Nb}$ , and  $^{197}\text{Au} + ^{197}\text{Au}$  at the balance energy for the hard equation of state (solid line) and HMD (dotted line). One notices that

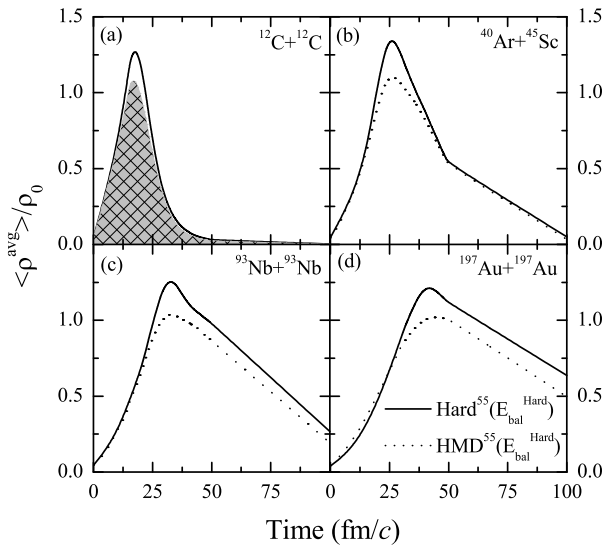


**Fig. 6.** Same as fig. 5, but for the average density ( $\langle \rho^{avg} \rangle / \rho_0$ ) versus reaction time.

the momentum-dependent interactions suppress the high dense phase of the reaction even at low incident energies like the balance energy. The reduction in the maximal value of the average density indicates a reduction in the number of nucleon-nucleon collisions. Note that the reduction in the maximal value of the average density is nearly the same in all the reactions irrespective of quite different energies of vanishing flow indicating nearly the same reduction in the number of binary nucleon-nucleon collisions and hence collision transverse flow for all the reacting systems. One also notices a faster decomposition of the compressed system using momentum-dependent interactions, as has been reported in ref. [7].

In our previous works [23], we had reported the mass dependence of the disappearance of transverse flow for the whole range from  $^{20}\text{Ne} + ^{27}\text{Al}$  to heavier masses ( $^{238}\text{U} + ^{238}\text{U}$ ). Our comparison with experimental data suggested a preference for the hard equation of state. Also nucleon-nucleon cross-sections of 35–40 mb explained the data throughout the mass range quite nicely. The experimental balance energy yielded  $\tau_{expt} = -0.42 \pm 0.05$ , whereas our results predicted  $\tau_{35} = -0.43 \pm 0.09$  and  $\tau_{40} = -0.42 \pm 0.08$  for the cross-sections of 35 and 40 mb, respectively. We here extend the above study to also include the  $^{12}\text{C} + ^{12}\text{C}$  reaction, therefore, increasing the mass range from 24 to 394. In addition, we shall also study the role of momentum-dependent interactions. In fig. 7, we display the balance energy as a function of the total mass of the system for  $^{12}\text{C} + ^{12}\text{C}$  to  $^{197}\text{Au} + ^{197}\text{Au}$ . We display the results for the hard equation of state (open square) and HMD (inverted triangles) with  $\sigma = 40$  mb. An enhanced nucleon-nucleon cross-section with  $\sigma = 50$  mb is also used in the case of momentum-dependent interactions (open hexagon). Experimental data are displayed by stars. The lines are the power law fits of the form ( $\propto A^\tau$ ). The dashed, dotted, dash-double-dotted and solid lines represent, respectively, the power law fit for  $\text{Hard}^{40}$ ,

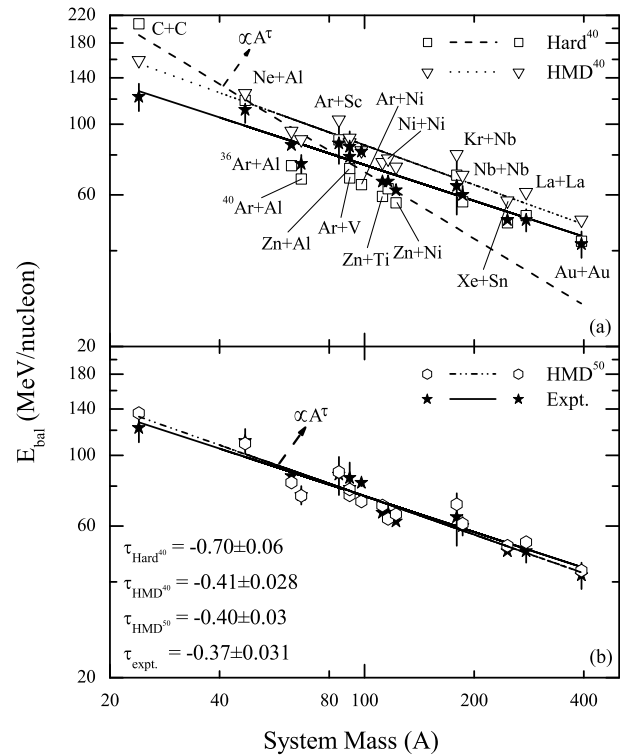


**Fig. 7.** (a) The balance energy as a function of the combined mass of the system. The experimental points along with error bars are displayed by solid stars. Our calculations for  $\sigma = 40$  mb with the hard (HMD) equation of state are represented by open squares (open down triangles). (b) Same as (a), but using HMD with  $\sigma = 50$  mb strength (denoted by open hexagons) and experimental data (denoted by solid stars). The lines are a power law fit of the form  $\propto A^\tau$ . The dashed, dotted and dash-double-dotted lines are the power law fit for  $\text{Hard}^{40}$ ,  $\text{HMD}^{40}$ , and  $\text{HMD}^{50}$ , respectively, whereas the solid lines represent experimental points.

$\text{HMD}^{40}$ ,  $\text{HMD}^{50}$ , and experimental data. The value of  $\tau$  for the experimental data is  $\tau_{expt} = -0.37 \pm 0.031$ , whereas  $\tau_{\text{Hard}^{40}} = -0.7 \pm 0.06$ ,  $\tau_{\text{HMD}^{40}} = -0.38 \pm 0.029$ , and  $\tau_{\text{HMD}^{50}} = -0.4 \pm 0.003$ . Once momentum-dependent interactions are included, the value of the  $\tau_{\text{HMD}^{40}}$  comes very close to the  $\tau_{expt}$  one. As noted in the upper part of the figure, the inclusion of momentum-dependent interactions improves the agreement for the  $^{12}\text{C} + ^{12}\text{C}$  system. One still notices that in most of the medium and heavy masses, it rather overestimates the balance energy. To improve the agreement further, we also simulated the reactions at  $\sigma = 50$  mb using momentum-dependent interactions. The comparison is displayed in the lower part of the figure. We see an excellent agreement of  $\text{HMD}^{50}$  with the experimental balance energy throughout the periodic table with mass between 24 and 394. Obviously, the effect is larger for lighter nuclei where the incident energy is higher compared to heavy nuclei having lower incident energies. The failure of the hard equation of state is due to the fact that it fails badly to explain the data for the  $^{12}\text{C} + ^{12}\text{C}$  reaction. It seems that the

static equation of state is not able to generate enough repulsion in terms of transverse momentum in lighter colliding nuclei. One should also note that the absolute values of the flow can also vary due to surface effects of a particular model. Though, as reported in ref. [23], other balance energies can be nicely explained. One possibility is to also use an enhanced cross-section for the static hard equation of state. This, however, worsen the balance energy agreement for medium and heavy nuclei.

## 4 Summary

Our present aim was to understand the impact and role of momentum-dependent interactions in the transverse flow and its disappearance observed in central heavy-ion collisions involving masses between 24 and 394, *i.e.*,  $^{12}\text{C} + ^{12}\text{C}$  and  $^{197}\text{Au} + ^{197}\text{Au}$ . We observed that the momentum-dependent interactions have a different impact in lighter colliding nuclei compared to heavier colliding nuclei. In lighter nuclei, the contribution of the mean field towards flow is much small compared to heavier nuclei, where binary nucleon-nucleon collisions dominate the scene. The inclusion of the momentum-dependent interactions also explains the energy of the vanishing flow in  $^{12}\text{C} + ^{12}\text{C}$  which otherwise was not possible with the static hard equation of state. The mass dependence of the balance energy was also studied with momentum-dependent interactions. We found an excellent agreement of our theoretical attempt with experimental data throughout the periodic table with masses between 24 and 394 units. Our present calculations suggested that if one wants to include  $^{12}\text{C} + ^{12}\text{C}$  also for the balance energy, momentum-dependent interactions are essential.

This work is supported by CSIR, Government of India under grant no. 7167/NS-EMR-II/2006.

## References

1. A. Akmal, V.R. Panharipande, D.G. Ravenhall, Phys. Rev. C **58**, 1804 (1998).
2. J. Aichelin, A. Rosenhauer, G. Peilert, H. Stöcker, W. Greiner, Phys. Rev. Lett. **58**, 1926 (1987).
3. C. Gale, G.F. Bertsch, S. Das Gupta, Phys. Rev. C **35**, 1666 (1987); C. Gale, G.M. Welke, M. Prakash, S.J. Lee, S. Das Gupta, Phys. Rev. **41**, 1545 (1990).
4. Q. Pan, P. Danielewicz, Phys. Rev. Lett. **70**, 2062 (1993).
5. J. Zhang, S. Das Gupta, C. Gale, Phys. Rev. C **50**, 1617 (1994).
6. D.T. Khoa, N. Ohtsuka, M.A. Matin, A. Faessler, S.W. Huang, E. Lehmann, R.K. Puri, Nucl. Phys. A **547**, 671 (1992).
7. B. Blättel, V. Koch, A. Lang, K. Weber, W. Cassing, U. Mosel, Phys. Rev. C **43**, 2728 (1991).
8. L.P. Csernai, G. Fal, C. Gale, E. Osnes, Phys. Rev. C **46**, 736 (1992).
9. V. de la. Mota, F. Sebille, M. Farine, B. Remaud, P. Schuck, Phys. Rev. C **46**, 677 (1992).
10. H. Zhou, Z. Li, Y. Zhou, G. Mao, Nucl. Phys. A **580**, 627 (1994).
11. M.J. Huang *et al.*, Phys. Rev. Lett. **77**, 3739 (1996).
12. F. Daffin, K. Haglin, W. Bauer, Phys. Rev. C **54**, 1375 (1996).
13. G.D. Westfall, Nucl. Phys. A **681**, 343c (2001).
14. H. Zhou, Z. Li, Y. Zhuo, Phys. Rev. C **50**, R2664 (1994).
15. S. Soff, S.A. Bass, C. Hartnack, H. Stöcker, W. Greiner, Phys. Rev. C **51**, 3320 (1995).
16. R. Pak, O. Bjarki, S.A. Hannuschke, R.A. Lacey, J. Lauret, W.J. Llope, A. Nadasen, N.T.B. Stone, A.M. Vander Molen, G.D. Westfall, Phys. Rev. C **54**, 2457 (1996).
17. E. Lehmann, A. Faessler, J. Zipprich, R.K. Puri, S.W. Huang, Z. Phys. A **355**, 55 (1996).
18. G. Peilert, H. Stöcker, W. Greiner, A. Rosenhauer, A. Bohnet, J. Aichelin, Phys. Rev. C **39**, 1402 (1989).
19. J.P. Sullivan *et al.*, Phys. Lett. B **249**, 8 (1990).
20. D. Krofcheck *et al.*, Phys. Rev. C **43**, 350 (1991).
21. Z.Y. He *et al.*, Nucl. Phys. A **598**, 248 (1996).
22. C. Hartnack, PhD Thesis, GSI Report **93**, 5 (1993).
23. A.D. Sood, R.K. Puri, Phys. Rev. C **69**, 054612 (2004); A.D. Sood, R.K. Puri, J. Aichelin, Phys. Lett. B **594**, 260 (2004).
24. G.D. Westfall *et al.*, Phys. Rev. Lett. **71**, 1986 (1993).
25. J.C. Angelique *et al.*, Nucl. Phys. A **614**, 261 (1997).
26. A. Buta *et al.*, Nucl. Phys. A **584**, 397 (1995).
27. D.J. Magestro, W. Bauer, G.D. Westfall, Phys. Rev. C **62**, 041603(R) (2000).
28. C.A. Ogilvie *et al.*, Phys. Rev. C **42**, R10 (1990).
29. D. Cussol *et al.*, Phys. Rev. C **65**, 044604 (2002).
30. R. Pak *et al.*, Phys. Rev. Lett. **78**, 1026; 1022 (1997).
31. D. Krofcheck *et al.*, Phys. Rev. C **46**, 1416 (1992).
32. W.M. Zhang *et al.*, Phys. Rev. C **42**, R491 (1990); M.D. Partlan *et al.*, Phys. Rev. Lett. **75**, 2100 (1995); P. Crochet *et al.*, Nucl. Phys. A **624**, 755 (1997).
33. D.J. Magestro, W. Bauer, O. Bjarki, J.D. Crispin, M.L. Miller, M.B. Tonjes, A.M. Vander Molen, G.D. Westfall, R. Pak, E. Norbeck, Phys. Rev. C **61**, 021602(R) (2000).
34. J. Aichelin, Phys. Rep. **202**, 233 (1991).
35. S. Kumar, M.K. Sharma, R.K. Puri, K.P. Singh, I.M. Govil, Phys. Rev. C **58**, 3494 (1998).
36. C. Hartnack, R.K. Puri, J. Aichelin, J. Konopka, S.A. Bass, H. Stöcker, W. Greiner, Eur. Phys. J A **1**, 151 (1998).
37. G.F. Bertsch, W.G. Lynch, M.B. Tsang, Phys. Lett. B **189**, 384 (1987).
38. H.M. Xu, Phys. Rev. Lett. **67**, 2769 (1991).
39. H.W. Barz, J.P. Bondorf, D. Idier, I.N. Mishustin, Phys. Lett. B **382**, 343 (1996).
40. B.A. Li, Z. Ren, C.M. Ko, S.J. Yennello, Phys. Rev. Lett. **76**, 4492 (1996).